Senckenbergiana maritima | 25 | (4/6) | 163–171 | Frankfurt am Main, 15. 5. 1995

Senckenberg am Meer 474

A Hydraulic Model for the Shore-normal Energy Gradient in the East Frisian Wadden Sea (Southern North Sea)

With 9 Text-Figures and 2 Tables

NTAHONDI NYANDWI & BURGHARD W. FLEMMING

Abstract

[NYANDWI, N. & FLEMMING, B. W. (1995): A hydraulic model for the shore-normal energy gradient in the East Frisian Wadden Sea (southern North Sea). — Senckenbergiana marit., 25 (4/6): 163–171, 9 figs., 2 tabs.; Frankfurt a. M.]

Sediment distribution maps of the East Frisian Wadden Sea show a clear tendency of fine sediment deposition in the vicinity of the mainland coast. At the same time a general seaward coarsening in grain sizes is documented, indicating the existence of a shore-normal energy gradient. An evaluation of the tidal prisms of E-W oriented channels and the subsequent estimation of their tidal discharges has allowed an estimation of the maximum attainable flow velocities of the individual channels. The results show that the maximum flow velocities decrease the closer a channel is situated to the mainland coast and that the velocity structure is controlled by the rate of rise of the tidal stage in a given channel and the topography of its catchment area.

These hydraulic relationships explain the nature of the linear, shore-normal energy gradient revealed in the grain size distribution patterns. The energy levels on the intertidal shoals between any two channels are primarily controlled by the flow structure of the channel situated to the north. By contrast, the flow in the adjacent southern channel is considerably weaker, thus influencing corresponding energy levels over a much shorter distance and time. This accounts for the strong segmentation of the otherwise linear energy gradient revealed in the cross-shore grain size patterns.

Introduction

The Wadden Sea is one of the most intensively studied coastal environments in the world and published data thus covers a wide range of topics and disciplines (e.g. BOEKSCHOTEN 1975; FLEMMING & HERTWECK 1994). One important feature that has been known at least since the 1950s is a general shoreward fining trend in the sediment distribution patterns, often culminating in thick mud deposits along the mainland coast of the Wadden Sea (e.g. VAN STRAATEN & KUENEN 1957, 1958; POSTMA 1957, 1961; FIGGE et al. 1980; FIGGE 1981; RAGUTZKI 1982; REINECK et al. 1986).

The enrichment of mud along the mainland coast was originally explained by the well-known **settling lag/scour lag model** of VAN STRAATEN & KUENEN (1958; see also POSTMA 1961). Initially it was thought that the relatively low concentrations of suspended sediment in the inlet mouths suggested a landward source. However, given the strong tidal flushing of the Wadden Sea, POSTMA (1961) concluded that a landward source was highly improbable and that the observed trend was indeed better explained by settling lag/scour lag effects. Some years later GROEN (1967) developed a model which showed that the landward transport of mud could also be explained by the asymmetry of the tidal flow. It is readily evident that the two models are mutually complementary.

Whereas the mechanisms outlined above can explain the landward transport and deposition of suspended sediments, they do not *per se* account for the shore-normal gradient observed in the coarser grain sizes on the basis of which the existence of a pronounced energy gradient across the backbarrier tidal flats was inferred (e.g. POSTMA 1967; FLEMMING & DAVIS 1994).

Authors' Addresses: N. NYANDWI, University of Dar Es Salaam, Institute of Marine Sciences, P. O. Box 668, Zanzibar, Tanzania. Present Address: c/o Forschungsinstitut Senckenberg, Schleusenstraße 39A, D-26382 Wilhelmshaven, Germany. — Dr. B. W. FLEMMING, Forschungsinstitut Senckenberg, Schleusenstraße 39A, D-26382 Wilhelmshaven, Germany.

The subtle nature of the grain size sorting patterns in the backbarrier tidal flats of the Wadden Sea has recently been documented by high-resolution settling velocity analyses (Bartholomä & Flemming 1994; Flemming & Ziegler 1995). This data have also revealed that the apparent depletion of fine-grained sediments in many parts of the Wadden Sea is the result of human interventions, induced by land reclamation and dike construction (Flemming & Nyandwi 1994), a process that is likely to be aggravated by the postulated acceleration in sea-level rise. In order to develop scientifically based management strategies these latest results urgently call for a hydraulic verification of the energy gradient model.

In the present study a hydraulic explanation is offered on the basis of spatial variations in flow velocities, coupled with the settling velocity characteristics of the non-cohesive component of the backbarrier sediments.

Geographic Setting

The East Frisian barrier island chain straddles the coast of northwest Germany between the Ems river mouth in the west and the outer Jade channel in the east. It forms part of the Frisian Islands that span the countries of The Netherlands, Germany and Denmark (e.g. Bartholdy & Pejrup 1994; Flemming & Davis 1994; Oost & de Boer 1994). The East Frisian island chain comprises seven major islands and several minor sandbanks (Fig. 1). The body of water separating the barrier islands from the mainland coast is generally referred to as the Wadden Sea. It is technically defined as that part of the coastal zone which is intermittently submerged and exposed by the rise and fall of the tides (e.g. Behre et al. 1979; Postma & Dijkema 1982; Ehlers 1988). The present study focusses on the catchment of the Otzum Inlet which is situated between the islands of Langeoog and Spiekeroog (Fig. 1).

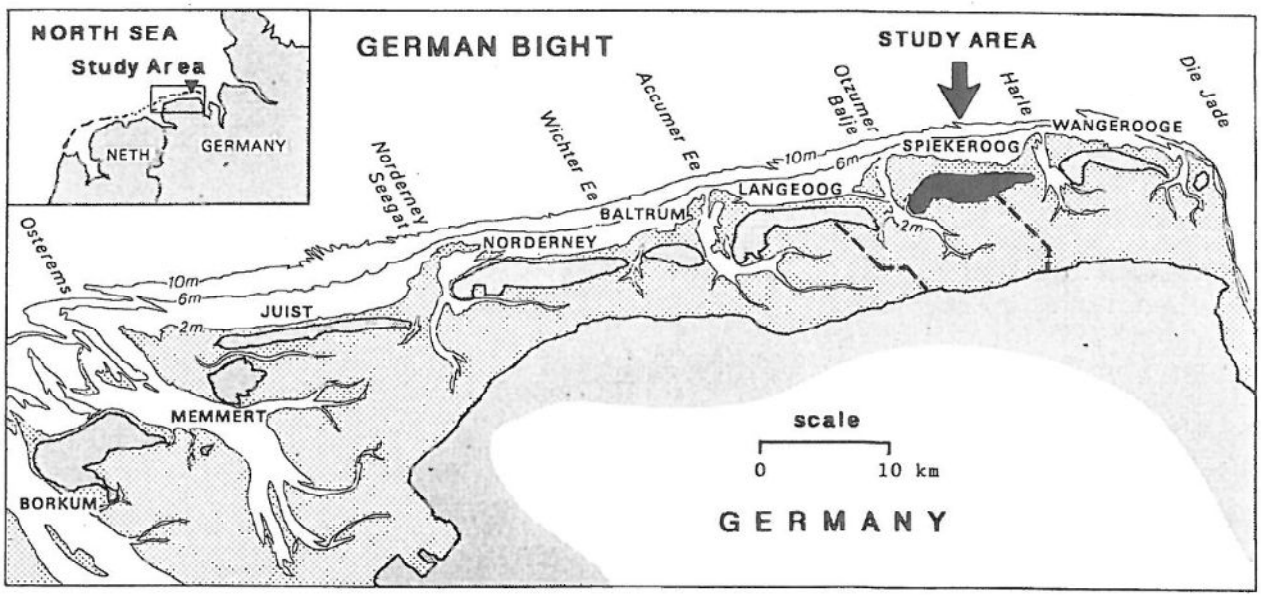


Fig. 1. Locality map of the East Frisian island chain, southern North Sea, showing the location of the study area.

Hydrographic Setting

The hydrodynamics of the Otzum catchment and the Wadden Sea on the whole is directly linked to the North Sea circulation regime which is mainly a result of the combined effects of tidal currents, atmospheric pressure fields, locally generated wind waves, and transmitted ocean swells from outside the region. The tidal water movements in the North Sea are driven by a system of three amphidromes (Huntley 1980), one situated in the north along the Norwegian coast, another in the central North Sea to the north of the German Bight (Fig. 2), and a third within the Southern North Sea Bight between The Netherlands and England.

The tidal circulation along the East Frisian barrier island chain is primarily controlled by the rotation of the tidal wave around the amphidromic point in the central North Sea, with a subordinate contribution of the southerly amphidrome, together resulting in an anti-clockwise motion of the M_2 tide (Fitzgerald & Penland 1987). In this way the tidal wave propagates eastwards along the East Frisian Islands and the more towards the east an island is

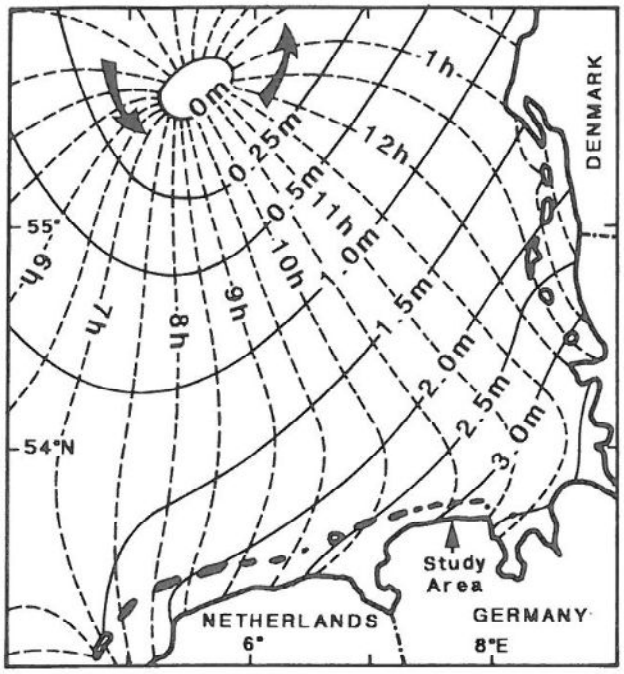


Fig. 2. The tidal amphidrome of the central North Sea showing corange and cotidal lines along the East Frisian islands. — After Flemming & Davis (1994).

situated, the greater is the delay in the time of high water (Fig. 2). Coupled with the orientation of the barrier island-chain this hydrographic regime leads to an increase in tidal range both from the north towards the islands and from west to east into the inner German Bight. Tidal ranges within the Wadden Sea basins, though much more modified by the local physiography, show a similar NW-SE increase in the tidal range as observed in the open North Sea (Fig. 3).

Tidal current measurements carried out in the back-barrier regions of Spiekeroog Island indicate velocities of 0.7–1.3 m s^{-1} in major channels (e.g. Davis & Flemming 1989; Bartholomä & Flemming 1993) and upto 0.3 m s^{-1} over intertidal flats (Bartholomä 1993). Together with the current data summarized by Fitzgerald & Penland (1987), published data from the island of Juist (e.g. Koch & Luck 1975), and unpublished data from the island of Norderney some insights into the temporal structure and scale of the flows are obtained. In general the tidal currents display a pronounced time-velocity asymmetry characterized by a shorter and faster flood phase. Current velocities are strongest near the inlet mouths and decrease towards the tidal drainage divides (e.g. Oost 1995). The larger eastern basins of the individual catchments are ebb-dominated, whereas the subordinate western basins are flood-dominated.

The tidal flows can be strongly modified by wind-driven currents. Winds blowing in the direction of the tidal current enhance the tidal flow and *vice versa,* at the same time causing substantial elevations or depressions of water levels along the coast. Current measurements at times of stormy weather reveal, among other things, an amplification of the ebb-current velocities of up to 60%, being coupled with a strong reduction in the duration of individual tidal phases (Koch & Niemeyer 1978).

An analysis of meteorological records from Norderney between 1965 and 1985 shows that 85% of the winds >10 Beaufort blow during the winter months, 30% of which occur in the month of November. These storm winds generally blow from the west, the northwest quadrant contributing 47%, followed by the western quadrant with 30%, the southwestern quadrant with 19% and the northern quadrant with 4% (Antia 1993). The resulting currents were shown to be strong enough to influence the morphodynamics of the tidal flats (e.g. Ehlers 1988).

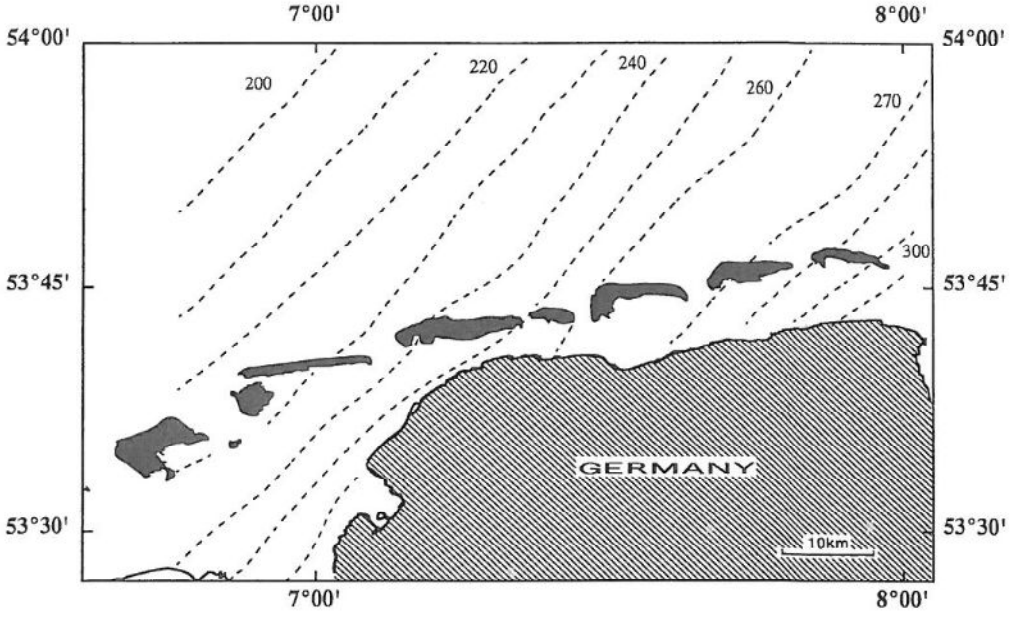


Fig. 3. Corange lines at 10 cm increments along the East Frisian coastline, southern North Sea, illustrating the southeastward increase in tidal range. — After Lassen (1989).

Sediment Distribution

Sediment maps of the East Frisian Wadden Sea have, over the years, been produced by a variety of federal and state authorities and research institutions, e.g. the Federal Geological Survey (SINDOWSKI 1966; BARCKHAUSEN et al. 1973), the German Hydrographic Institute (FIGGE 1981), the Coastal Research Laboratory on Norderney (RAGUTZKI 1982; GROTJAHN 1990), and the Senckenberg Institute in Wilhelmshaven (e.g. REINECK et al. 1986; FLEMMING & NYANDWI 1994; FLEMMING & ZIEGLER 1995).

These maps show that up to 60% of the sediment consists of fine sand. The mud content (grain sizes <0.063 mm or >4.0 phi) generally increases towards the mainland coast but rarely exceeds 30%, except in local embayments where values >50% can be recorded. Coarser sediments are restricted to the deeper channels, gravel and bedrock outcrops being only found in the Weser and Ems estuaries. Unfortunately, most of the sediment maps are not directly comparable with each other since different methods of grain size analysis, as well as different classification schemes have been used (FLEMMING & ZIEGLER 1995).

Based on petrographic and mineralogic analyses carried out in the 1950s, it was concluded that most of the sediment found in the Wadden Sea probably originated from the North Sea (VAN STRAATEN & KUENEN 1957). Nevertheless, sediment sources other than the North Sea have also been considered. The fine-grained sediments found in the inner German Bight, for example, are thought to have been derived, at least in part, from the Weser and Elbe rivers, as well as from the North Frisian Wadden Sea in the course of storm surges (REINECK et al. 1967, 1968; GADOW & REINECK 1969). For the purpose of the present study, the sediment data of the Senckenberg Institute was used as it is the only data derived from high-resolution settling velocity analyses (FLEMMING & DAVIS 1994; FLEMMING & ZIEGLER 1995).

Results

The Energy Gradient

In order to better resolve the shore-normal energy gradient, about 2000 sediment samples were collected on a closely spaced grid (280 m × 280 m) in the backbarrier tidal flats of Spiekeroog Island (Fig. 4). The mud fraction of the collected samples was removed and expressed as a percentage of the bulk sample. The remaining sand fraction was processed through a high-resolution settling tube to obtain settling velocity distributions, equivalent settling diameters, as well as their respective statistical parameters.

The spatial distribution map of mean settling diameters shows a distinct segregation of individual size classes, the

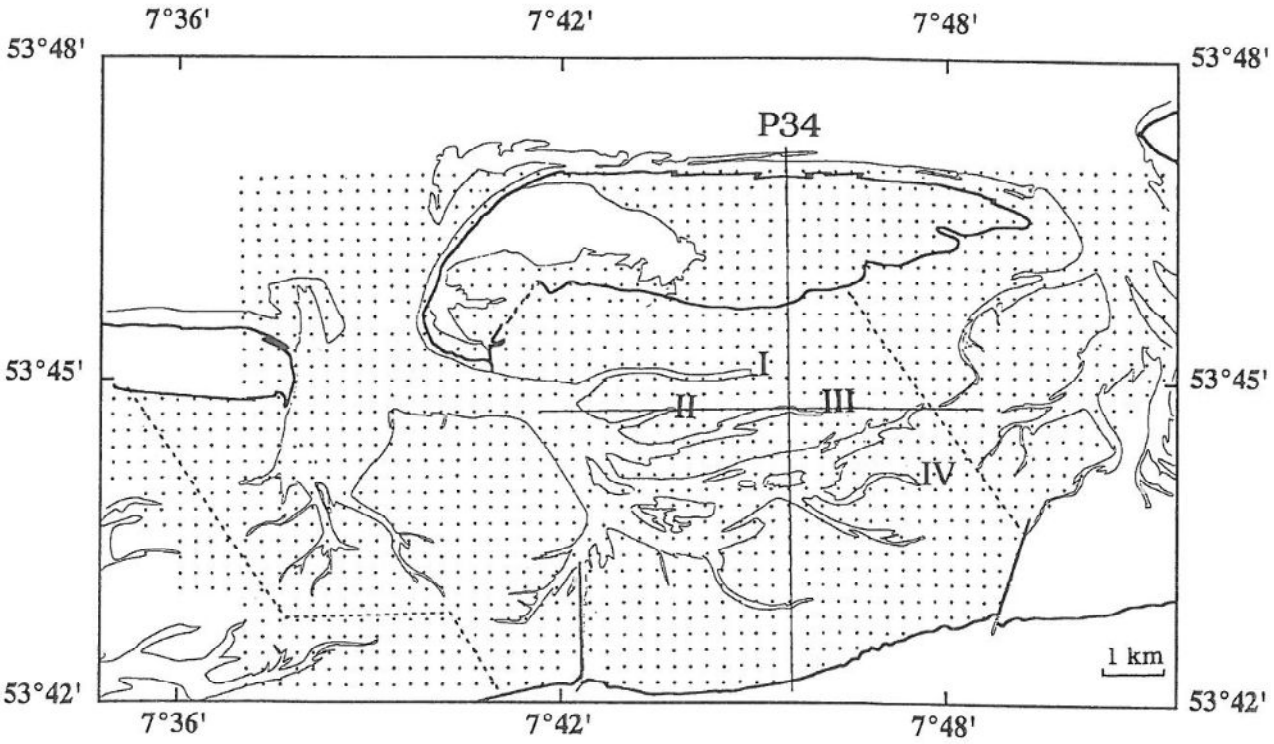


Fig. 4. Sample grid and general drainage pattern of the Otzum tidal basin catchment, southern North Sea.

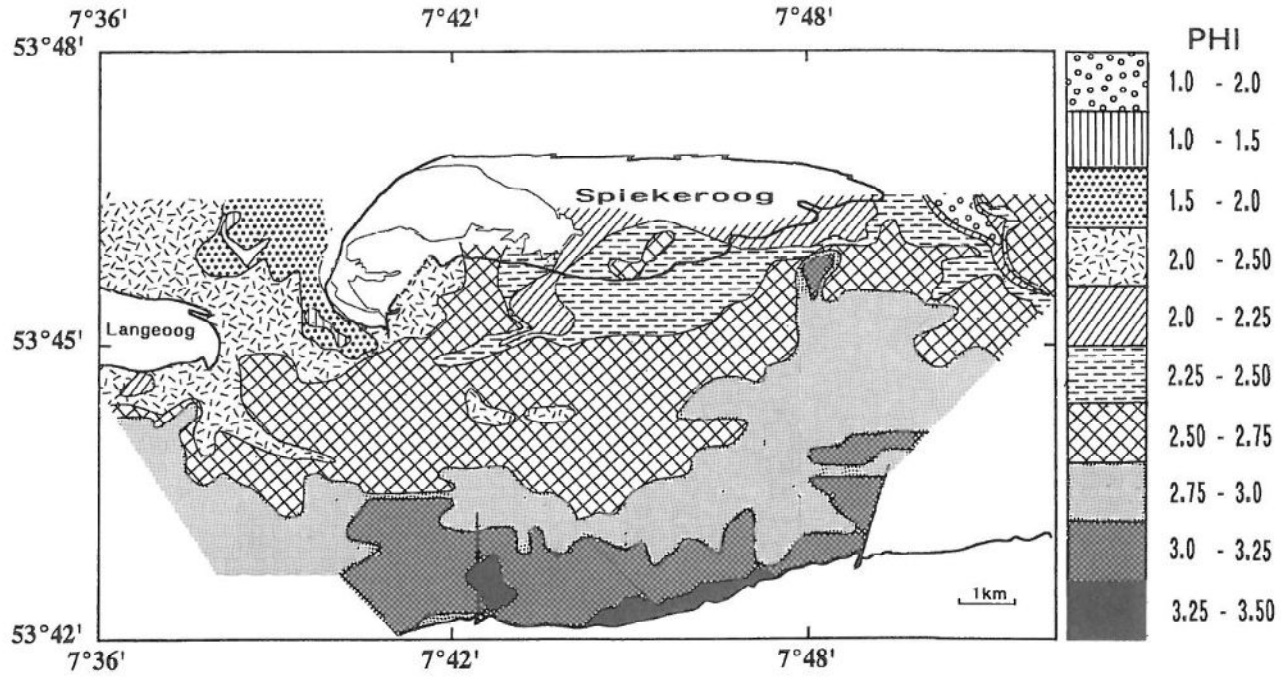


Fig. 5. Spatial distribution of mean grain sizes in the study area of Spiekeroog Island, southern North Sea.. — Note the cross-shore grain size gradient reflecting a shore-normal energy gradient.

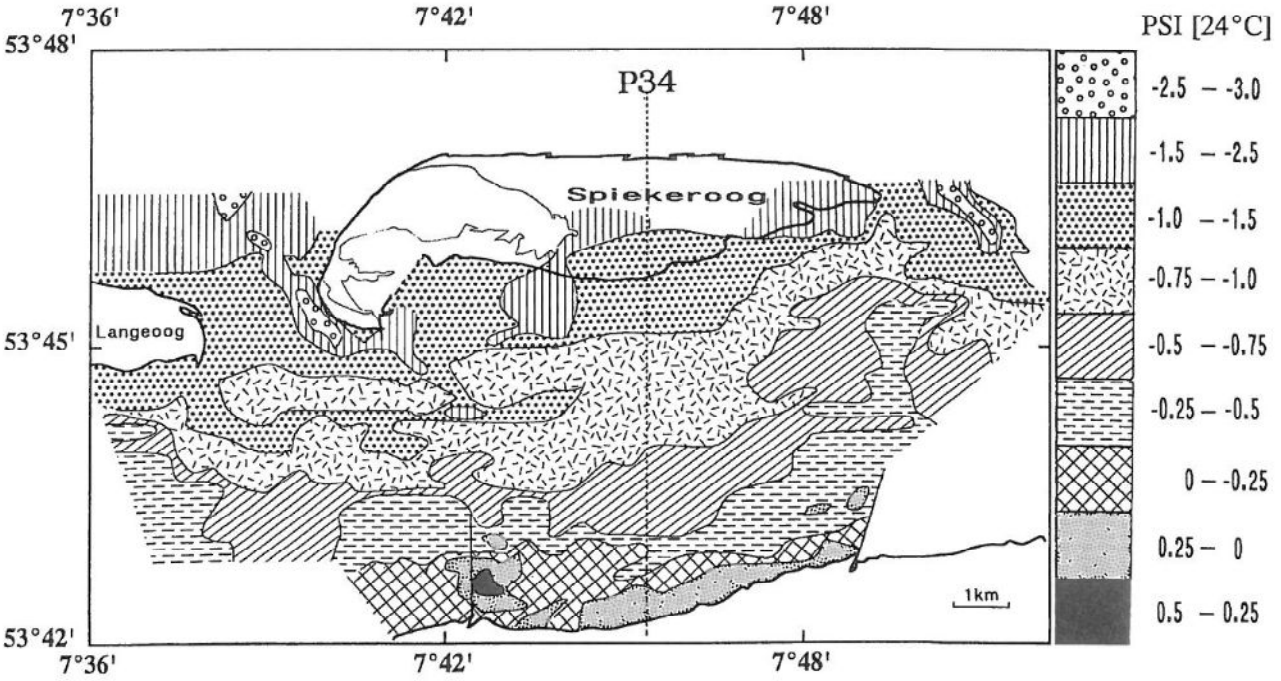


Fig. 6. Spatial distribution of mean grain settling velocities. — Note the close resemblance with Fig. 5. — Spiekeroog Island area, southern North Sea.

sediment being finest (3.25–3.5 phi) near the dike and coarsest along the seaward boundary of the study area (Fig. 5). A similar differentiation is obtained when plotting mean grain settling velocities (Fig. 6). Both patterns reflect a shoreward decreasing energy gradient. This gradient can be represented by plots of median grain sizes, mean grain sizes, modal grain sizes, or mean settling velocities as a function of the shore-normal distance across the backbarrier tidal flats. A plot of successive high-resolution frequency curves, for example, clearly demonstrates the modal shift along the N-S gradient (Fig. 7).

When plotting the progression of mean grain settling velocities with distance along the cross-shore transect, a highly correlated linear relationship is obtained ($r = 0.83$) (Fig. 8), thus proving the existence of a corresponding linear, shore-normal energy gradient. By contrast, the frequency curves along shore-parallel transects do not reveal an E-W gradient, as the shape of the tidal basin and the E-W orientation of some tidal channels might have suggested (Fig. 7).

Tidal Prism, Basin Structure and Tidal Discharge

Tidal currents and wave action constitute the major hydraulic forces in tidal environments. In the study area, these forces must evidently change in a systematic manner in correspondence to the shore-normal energy gradient inferred from the grain size pattern (VAN STRAATEN & KUENEN 1958). Considering the E-W orientation of some channels, the energy gradient would suggest that the discharges of the subcatchments corresponding to these channels should increase the farther a channel is situated from the mainland coast. The associated flow strength, however, is not only controlled by the tidal prism of a subcatchment, but also by the channel form and basin structure (topography).

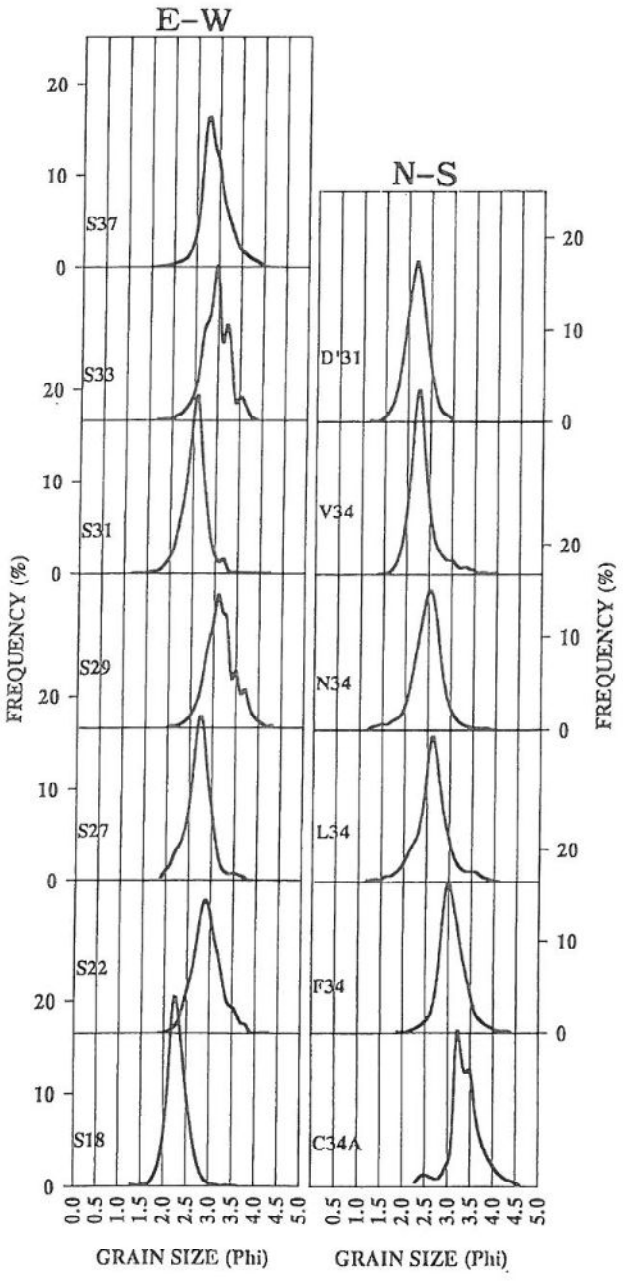


Fig. 7. Sequence of grain size frequency curves along N-S and E-W transects. — Note the systematic modal shift along the postulated energy gradient for the N-S transect and the absence of a clear grain size sorting trend along the E-W transect. — Spiekeroog Island area, southern North Sea.

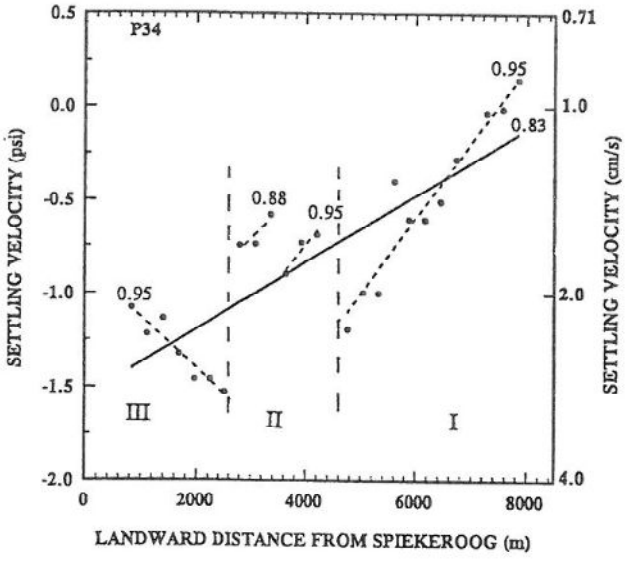


Fig. 8. Mean grain settling velocities as a function of cross-shore distance. — The broken line segments represent descrete energy zones along the general shore-normal energy gradient represented by the thick regression line. — Zone I: near-dike flats; Zone II: interchannel flats; Zone III: backbarrier shore and adjacent flats. — Spiekeroog Island area, southern North Sea.

Tidal Discharge

The tidal filling process of the backbarrier basins can be considered as a tidal pumping through the inlet and subsequent tidal channels. The discharge of channels with rectangular plan forms can be calculated on the basis of equations representing the horizontal (Q_H) and the vertical discharge (Q_V), respectively:

$$Q_H = A_c \times V \quad (1)$$

$$Q_V = A_p \times dH/dT \quad (2)$$

where V is the flow velocity, A_c is the cross-sectional area, A_p is the basin surface area, and dH/dT is the rate of rise of the tidal stage. Applying the law of continuity ($Q_H = Q_V$), then

$$A_c \times V = A_p \times dH/dT \quad (3)$$

and

$$V = (A_p/A_c) \times dH/dT \quad (4)$$

Tidal Prism and Basin Structure

Because the shapes of the tidal channels do in reality not correspond to rectangular basins and their banks do not rise up to the high water mark, some of the flow is actually overbank and the rate of water level rise (dH/dT) and the surface area (A_p) are, in addition, controlled by the basin structure (topography). The channel cross-sectional area is the only variable remaining constant at bankfull discharge. The additional tidal water demand, which is brought about by increasing tidal stages above the channel banks, must thus be compensated by an increased discharge. This results in velocity surges at the channel entrances.

In this case, the flow velocity (equation 4) has to be calculated and summed at discrete time intervals, thus accounting for the contributions to the tidal prism by different stage elevations. Taking A_p to represent the surface area of the channel at chart datum and A_{ip} the surface area of any other level H_i, then

$$V = 1/A_c[A_p(dH/dT) + \Sigma(A_{ip} \times dH_i/dT)] \quad (5)$$

Maximum Flow Velocities

In order to calculate the flow velocities on the basis of equation (5) as accurately as possible, a large scale (1 : 25,000) topographic map of the study area was digitized. A number of tidal channels (numbered I–IV in Fig. 5) occupying different grain size zones and having clearly demarcated catchment areas were then selected and their surface areas at chart datum measured. In addition, the surface areas between selected contour intervals, i.e. NN + 0, NN + 0.25 and NN + 1.0 m, as well as the mean high water mark at NN + 1.3 m were evaluated. A time interval (dT) of 6 hours was used, assuming a time symmetry of the tides. The computational details and results are summarised in Tabs. 1–2.

From the computational results it can be seen that the predicted flow velocities are highest in the northernmost channel (I), followed in geographic sequence by channel II, III and IV. The flow velocities and hence the energy levels thus clearly increase along a shore-normal, i.e. N-S gradient.

Table 1. Hydraulic parameters for the computation of equlibrium flow velocities in local tidal channels. — Spiekeroog Island area, southern North Sea.

Channel No.	I	II	III	IV	
H_i (m)	A_{hi} (km²)	A_{hi} (km²)	A_{hi} (km²)	A_{hi} (km²)	dH_i/dT (mm s⁻¹)
-1.5	0.477	0.105	0.919	0.228	0.13
0	4.734	0.923	4.110	1.044	0.06
0.25	4.837	1.071	4.186	-	0.05
1.0	7.465	-	-	-	0.01

Table 2. Computed equilibrium flow velocities as a function of cross-sectional channel area. — Spiekeroog Island area, southern North Sea.

Channel No.	X-Sectional area (m²)	$V=1/A(\Sigma A_{hi}\, dH_i/dT)$ (m s⁻¹)
I	305.879	1.18
II	90.270	0.78
III	451.407	0.70
IV	125.504	0.69

Discussion

The agreement between the gradients of the estimated maximum channel velocities and the mean grain settling velocities (Fig. 9) clearly validates the proposed causal relationship between the tidal flow velocity and surficial sediment distribution. The velocity gradient implies that overbank flow velocities between any two adjacent chan-

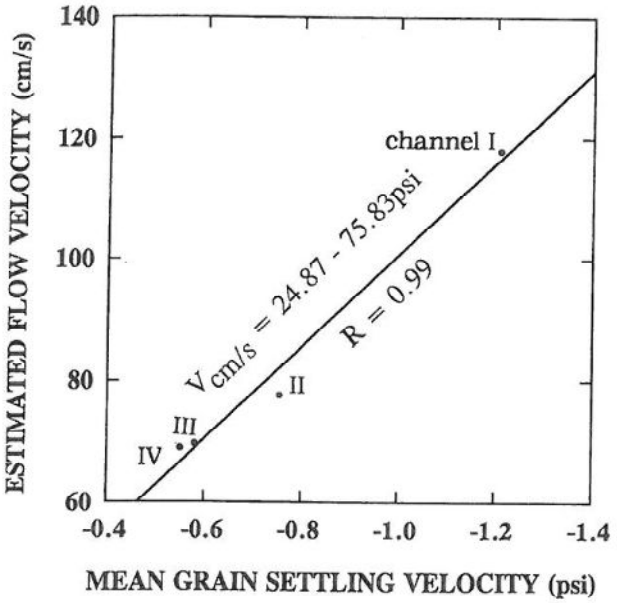


Fig. 9. Correlation between the grain settling velocities and predicted maximum flow velocites of E-W oriented channel systems (channel I lies in the north, channel IV in the south). — The good correlation indicates a causal relationship. — Spiekeroog Island area, southern North Sea.

nels will be influenced over a large distance by the velocity structure of the channel situated to the north. The channel situated to the south will therefore only be able to slightly modify that effect, a feature that can explain the scatter in the data points from the interchannel region of the energy gradient (Fig. 8).

Whereas this interpretation is able to explain the observed energy gradient and the resulting grain size pattern, certain depositional features, e.g. the occurrence of muds on intertidal flats away from the mainland dike (Flemming & Davis 1994; Flemming & Nyandwi 1994; Flemming & Ziegler 1995) would seem to contradict the energy gradient model. It has been demonstrated, however, that the origin of these muds are mostly controlled by site specific factors such as biosedimentation in and around mussel beds (van Straaten & Kuenen 1958; Flemming 1990; Flemming & Delafontaine 1994) and topographic effects (Reineck et al. 1986).

Finally, short-lived events such as storms, or seasonal effects caused by temperature related differences in settling velocities of the sediment, are expected to introduce a local "noise factor" into the energy gradient and hence also the sediment zonation pattern. This should be reflected in slight variations of mean grain sizes when monitored over seasonal time scales.

Conclusions

Mathematically derived hydraulic predictions have been used to explain the actual cause of the shore-normal energy gradient observed in the East Frisian Wadden Sea on the basis of grain size distribution patterns.

Whereas the tidal inlets generally trend NW-SE, their tributaries have E-W to NE-SW orientations such that they run more or less parallel to the trend of the coastline. The size and structure of the subcatchments associated with each of these shore-parallel channels determines the size of their respective tidal prism and the rate of rise of the tidal levels, thereby determining their maximum discharge velocities.

The channel to channel variation of the tidal prism results in a progressive southward decrease in discharge velocities from one channel to the next, thereby defining a general shore-normal energy gradient. This, in turn, explains the observed cross-shore grain size distribution pattern, including its local segmentation.

Acknowledgements

The authors wish to express their gratitude to the Deutscher Akademischer Austauschdienst (DAAD) and the Senckenbergische Naturforschende Gesellschaft (SNG) for providing financial and logistical support.

References

Antia, E. E. (1993): Sedimentology, morphodynamics and facies association of a mesotidal barrier island shoreface (Spiekeroog, southern North Sea). — Ber. Fachbereich Geowiss. Univ. Bremen, 32: 370 pp.

Barckhausen, J. & Lang, H. D. & Mengeling, H. & Meyer, K.-D. & Streif, H. & Elwert, D. (1973): Geologische Übersichtskarte 1:200 000, Blatt CC 2310 Helgoland. — Bundesanstalt für Bodenforschung, Hannover.

Bartholdy, J. & Pejrup, M. (1994): Holocene evolution of the Danish Wadden Sea. — Senckenbergiana marit., 24: 187–209.

Bartholomä, A. (1993): Zeitliche Variabilität und räumliche Inhomogenität in den Substrateigenschaften und der Zoobenthosbesiedlung im Umfeld von Miesmuschelbänken. D. Hydrodynamik. — Ber. Senckenberg am Meer, 93/1: 117–123.

Bartholomä, A. & Flemming, B. W. (1993): Zeitliche Variabilität in den Sedimentparametern und der Morphologie auf der Gröninger Plate (Spiekerooger Watt). — Ber. Senckenberg am Meer, 93/1: 54–48.

— — — (1994): Massenbilanz und Transportsortierung der Sedimente auf der Gröninger Plate. — In: Umweltbundesamt [Ed.]: Berichte aus der Ökosystemforschung, 4 (2): 218–220.

Behre, K.-E. & Menke, B. & Streif, H. (1979): The Quaternary development of the German part of the North Sea. — In: Oele, E. & Schüttenhelm, R. T. E. & Wiggers, A. J. [Eds.]: The Quaternary History of the North Sea. — Acta Universitatis Upsaliensis, Symposium Annum Quingentesimum Celebrantis, 2: 85–113.

Boekschoten, M. (1975): Liste von Veröffentlichungen über das Wattenmeer. — Rijksinstituut voor Natuurbeheer: 191 pp.; Leersum, The Netherlands.

Davis, R. A., Jr. & Flemming, B. W. (1989): Time-series study of mesoscale tidal bedforms, Martens Plate, Wadden Sea, Germany. — Mem. Canad. Soc. Petroleum Geologists, 16: 275–282.

Ehlers, J. (1988): Morphodynamics of the Wadden sea. — 397 pp,; Rotterdam (Balkema).

Figge, K. (1981): Sedimentverteilung in der Deutschen Bucht, Blatt Nr. 2900. — Hamburg (Deutsches Hydrographisches Institut).

Figge, K. & Köster, R. & Thiel, H. & Wieland, P. (1980): Schlickuntersuchungen im Wattenmeer der Deutschen Bucht. — Die Küste, 35: 147–186.

Fitzgerald, D. M. & Penland, S. (1987): Backbarrier dynamics of the East Frisian islands. — J. Sediment. Petrol., 54 (4): 746–754.

Flemming, B. W. (1990): Zur holozänen Entwicklung, Morphodynamik und faziellen Gliederung der mesotidalen Düneninsel Spiekeroog (südliche Nordsee). — Ber. Fachbereich Geowiss. Univ. Bremen, 10: 13–73.

Flemming, B. W. & Davis, R. A., Jr. (1994): Holocene evolution, morphodynamics and sedimentology of the Spiekeroog barrier island system (southern North Sea). — Senckenbergiana marit., 24: 117–155.

Flemming, B. W. & Delafontaine, M. T. (1994): Biodeposition in a juvenile mussel bed of the East Frisian Wadden Sea (southern North Sea). — Netherl. J. aquat. Ecol., 28: 289–297.

Flemming, B. W. & Hertweck, G. [Eds.] (1994): Tidal Flats and Barrier Systems of Continental Europe. A Selected Overview. — Senckenbergiana marit., 24: 1–209.

Flemming, B. W. & Nyandwi, N. (1994): Land reclamation as a cause of fine-grained sediment depletion in backbarrier tidal flats (southern North Sea). — Netherl. J. aquat. Ecol., 28: 299–307.

Flemming, B. W. & Ziegler, K. (1995): High-resolution grain size distribution patterns and textural trends in the backbarrier region of Spiekeroog Island, southern North Sea. — Senckenbergiana marit., 26: (in press).

Gadow, S. & Reineck, H.-E. (1969): Ablandiger Sandtransport bei Sturmfluten. — Senckenbergiana marit., [1] 50: 63–78.

Groen, P. (1967): On the residual transport of suspended matter by an alternating tidal current. — Netherl. J. Sea Res., 3: 564–574.

Grotjahn, M. (1990): Sedimente und Mikrofauna der Watten bei der Insel Spiekeroog. Untersuchungen im Rahmen des „Sensitivitätesrasters Deutsche Nordsee-Küste". — Jber. 1987 Forschungsstelle Küste, Norderney, 39: 97–119.

Huntley, D. A. (1980): Tides in the North-West European continental shelf. — In: Banner, F. T. & Collins, M. B. & Massie, K. S. [Eds.]: The North-West European Shelf Seas: The Sea in Motion II. Physical and Chemical Oceanography, and Physical Resources: 301–351; Amsterdam (Elsevier).

Koch, M. & Luck, G. (1975): Untersuchung zu den Strömungsverhältnissen auf dem westlichen Juister Watt. — Jber. 1974 Forschungsstelle Insel- u. Küstenschutz, Norderney, 26: 29–31.

Koch, M. & Niemeyer, H. D. (1978): Sturmtiden-Strommessungen im Berreich des Norderneyer Seegats. — Jber. 1977 Forschungsstelle Insel- u. Küstenschutz, Norderney, 29: 91–108.

Lassen, H. (1989): Örtliche und zeitliche Variationen des Meeresspiegels in der südöstlichen Nordsee. — Die Küste, 50: 65–95.

Oost, A. P. (1995): Sedimentological implications of morphodynamic changes inthe ebb-tidal delta, the inlet and the backbarrier environment of the Zoutkamperlaag tidal inlet (Dutch Wadden Sea), induced by a sudden decrease inthe tidal prism. — Spec. Publ. internat. Assoc. Sedimentologists, 24: (in press).

Oost, A. P. & Boer, P. L. de (1994): Sedimentology and development of barrier islands, ebb-tidal deltas, inlets and backbarrier areas of the Dutch Wadden Sea. — Senckenbergiana marit., 24: 65–115.

Postma, H. (1957): Size frequency distribution of sands in the Dutch Wadden Sea. — Arch. Néerl. Zool., 12: 319–349.

— — — (1961): Transport and accumulation of suspended matter in the Dutch Wadden Sea. — Netherl. J. Sea Res., 1: 148–190.

Postma, H. & Dijkema, K. S. (1982): Hydrography of the Dutch Wadden Sea: Movements and properties of water and particulate matter. — Final Report on 'Hydrography' of the Wadden Sea Working Group, Rep. 2: 75 pp.; Rotterdam (Balkema).

Ragutzki, G. (1982): Verteilung der Oberfläschensedimente auf den Niedersächsischen Watten. — Jber. 1980 Forschungsstelle Insel- u. Küstenschutz, Norderney, 32: 55–67.

Reineck, H.-E. & Chen, C. M. & Wang, S. S. (1986): Die Rückseitenwatten zwischen Wangeroog und Festland, Nordsee. — Senckenbergiana marit., 17: 241–252.

Reineck, H.-E. & Dörjes, J. & Gadow, S. & Hertweck, G. (1968): Sedimentologie, Faunazonierung und Faziesabfolge vor der Ostküste der inneren Deutschen Bucht. — Senckenbergiana lethaea, 49 (4): 261–309.

Reineck, H.-E. & Gutmann, W. F. & Hertweck, G. (1967): Das Schlickgebiet südlich von Helgoland als Beispiel rezenter Schelfablagerungen. — Senckenbergiana lethaea, 48 (3/4): 219–275.

Sindowski, K.-H. (1966): Geologische Karte von Niedersachsen 1:25 000, Blatt 2212 Spickeroog. — Niedersächsisches Landesamt für Bodenforschung, Hannover.

Straaten, L. M. J. U. van & Kuenen, P. H. (1957): Accumulation of fine grained sediment in the Dutch Wadden Sea. — Geol. en Mijnbouw, 19: 329–354.

— — — & — — — (1958): Tidal action as a cause of clay accumulation. — J. sediment. Petrol., 28 (4): 406–413.